Multiple-scattering theories including correlation effects to obtain the effective dielectric constant of nonhomogeneous thin films

Manuel Gómez, Luis Fonseca,* Gerardo Rodríguez,† Angel Velázquez, and Luis Cruz
University of Puerto Rico, Río Piedras, Puerto Rico
(Received 28 January 1985)

Existing theories for the effective optical properties of a ceramic-metal granular medium (cermet) are discussed within a multiple-scattering analysis and used as the starting point for including correlation effects. Analysis of the nucleation and growth process in cermets indicates that the correlation between the islands of the less abundant material are important in the study of optical properties. Multiple-scattering corrections are considered by solving the field equation in the first smoothing approximation. The results obtained with this model are compared with other theories and against experimental data of real cermets. Quantum-size-effect corrections to the dielectric constant of the metallic grains in dielectriclike cermets and their effect on the results of the theory are also analyzed. Finally, renormalization effects introduced through a T-matrix formalism are discussed. Comparison between the results of the proposed model and the experimental data for different cermets shows that the theory developed has better predictive value than earlier models and good agreement is obtained with experiment even when the metal concentration is large.

I. INTRODUCTION

Cermets are inhomogeneous materials consisting of immiscible mixtures of insulators (i.e., ceramics) and metals. The optical properties of cermets have been extensively researched because of their potential application to the development of optically selective surfaces.[1] Considerable work has been performed to develop theoretical models which will correctly predict the optical properties of cermets when the bulk dielectric constant of the constituents is known experimentally. It has been found that the optical properties of cermets can be modified by changes in the relative concentration of the constituents and the concomitant change in microstructure.[2] Based on constituent concentration, cermets are classified into three general types: (a) metallic cermets, where the dominant volume fraction is metallic and, as a consequence, metallic properties dominate the optical properties of the material; (b) dielectric cermets, where the dielectric constituent is dominant and, as a result, metallic inclusions are formed in a dielectric matrix; (c) intermediate cermets, where an interconnected metallic network develops—in this region percolation effects are observed.[3] At opposite extremes when the volume fraction of the metallic or dielectric constituents is very high ($\sim 98\%$), the optical properties are determined by the major constituent. But when the concentration of the dominant constituent is less than 98%, the material develops a distinct resonance which is not characteristic of either one of the constituents. The prediction of this resonance has been the goal of all theories developed for the optical properties of cermets.

Since for the region of interest in the electromagnetic spectrum the wavelength of the radiation is large compared to the metallic islands, an electrostatic approximation can be made. In this regime a simple relation between the internal ($\mathbf{E}_{\text{in}}$) and the external ($\mathbf{E}_{\text{out}}$) electric fields for a single spherical island can be made, yielding the relationship[4]

$$\mathbf{E}_{\text{in}} = \frac{3}{2+\epsilon(\omega)}\mathbf{E}_{\text{out}} ,$$

which predicts a resonance when the dielectric constant $\text{Re}\epsilon(\omega) = -2$. Essentially this singularity is responsible for the resonance structure in cermets.

The technological usefulness of cermets when applied to optical devices comes from their optical response in the region $0.8\ \mu\text{m} < \lambda < 2.5\ \mu\text{m}$. Since in the spectral region of interest the wavelength is larger than the microstructure, an effective-medium dielectric constant can be used to characterize the optical response of the materials. Based on this idea, several theoretical models have been proposed to obtain the effective dielectric constant of cermets in terms of the dielectric constant of the constituents and other parameters describing the microstructure, such as island radii, relative concentrations of the constituents, and the shape of the islands. Two basic and widely used models are the Maxwell-Garnett (MG) and the Bruggeman (B) models.[5] The MG model is asymmetric, since it considers the cermet as being composed of the less abundant constituent embedded in a matrix of the most abundant material. The effective dielectric constant is then obtained by performing a volume average over the local fields. While the B model is symmetric, since it considers the two constituent materials as spheres embedded in an effective medium, a volume average is also performed to obtain a self-consistent expression for the effective dielectric constant. In both theories a resonance in the spectral response of the cermet is obtained, but neither result agrees with the experimentally measured complex dielectric constant (Fig. 1). For example, comparison between the experimentally obtained imaginary part of the effective index of refraction and the MG model reveals that

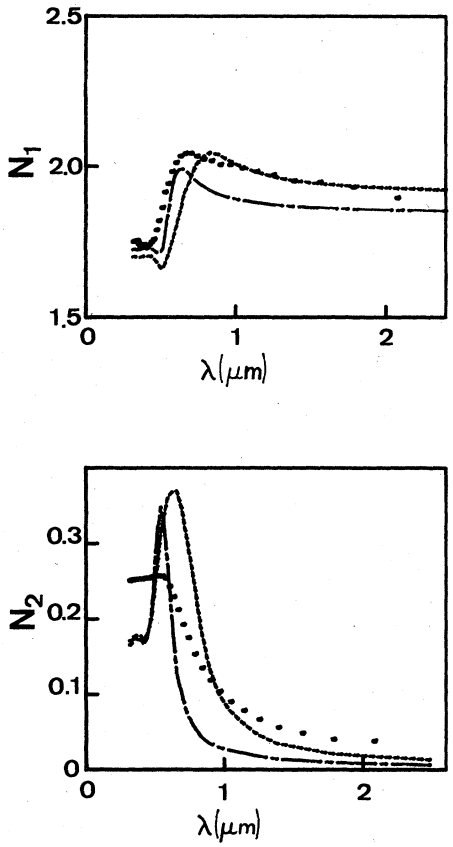

FIG. 1. Real (N_1) and imaginary (N_2) parts of the index of refraction for Au-Al_2O_3 (90 vol% Al_2O_3) using the Drude model with an effective mean free path of 10 Å. Dashed curve represents the B calculation, the dashed-dotted curve is the MG, and the dots are experimental data from Craighead (Ref. 21).

the theoretical resonance is too narrow and in many cases blue-shifted with respect to experimental results. Several papers, like those of Granqvist,[6] show that the magnitude and position of the resonance is a strong function of the inclusion's shape. Corrections to the dielectric constant of metallic grains for size effects have been extensively used to reduce the magnitude of the resonance, but they fail to produce enough red shift and broadening to explain experimental data.

The objective of this paper is to show that corrections due to the correlation between the position of the metallic islands, resulting from the formation process of the cermet, can move and broaden the resonance obtained by the traditional mean-field theories of Maxwell-Garnett and Bruggeman. In order to perform this correction, a multiple-scattering theory has been developed that starts from an effective dielectric constant that is calculated assuming no correlation between the metallic islands and labeled in this work as the zeroth-order approximation. Nonrenormalized and renormalized theories will be discussed in which correlation effects are taken into account. The final result for the effective dielectric constant will be expressed in terms of the zeroth-order effective dielectric constant $\bar{\epsilon}_0$ (which contains no correlation effects but has been renormalized), the relative concentration of the constituents f, the dielectric constant of the less abundant constituent corrected for size effects ϵ_m, the radius of the inclusions a, and a correlation length L.

Existing theories, including those that take into account the shape of the islands in an effort to improve the predicted value of the mean-field theories will be analyzed and discussed. Also corrections for size effects to the dielectric constant of the metallic grains will be studied and it will be shown that it is necessary to take into account quantum size effects for metallic islands of good metals with radii less than 100 Å.

A. Mean-field models

In order to explain the characteristic resonance peak of cermets and other nonhomogeneous media two basic mean-field models have been proposed by Maxwell-Garnett and Bruggeman. Many derivations of these theories have been made by several authors,[7,8] and it has been shown that the MG theory is a zeroth-order approximation of more complex multiple-scattering theories.[9,10] The authors have been able to show that the Bruggeman theory can also be reduced to the zeroth-order approximation in a multiple-scattering formulation of the problem. Both theories are effective-medium theories within the electrostatic approximation and are obtained from volume averages. The Maxwell-Garnett theory is an asymmetric model considering the cermet as being composed of islands of the less abundant constituent embedded in a matrix of the most abundant material, while the Bruggeman model is a self-consistent theory and assumes that both constituents form spheres that are surrounded by the effective medium. The response of islands in the cermet to an external electric field produces a resonance in the complex dielectric constant. In general, the Maxwell-Garnett theory produces resonance peaks that are too narrow and usually shifted towards the blue region of the spectrum with respect to the experimental results, while the Bruggeman theory tends to underemphasize the structure.

Several modifications have been performed in an attempt to obtain better agreement with experimental results. In particular, considerable effort has been invested in correcting the theory for effects of changes in the shape of the islands in the cermet.[11] Granqvist[6] has taken into consideration not only shape effects, but the contribution of chains, double spheres, fcc clusters, and even combinations of these shapes in order to bring mean-field-theory calculations closer to experimental results. In particular, he calculates the logarithm of the transmission for metallic-type cermet (Ag-SiO_2, 17 vol% SiO_2) using the MG model, under the assumption that the dielectric inclusions are ellipsoids instead of spheres, and expressing the effective dielectric constant as

$$\bar{\epsilon}_{\mathrm{MG}}=\epsilon_{\mathrm{ma}}\frac{1+\frac{2}{3}f\alpha}{1-\frac{1}{3}f\alpha},$$

where ϵ_{ma} is the bulk dielectric constant of the matrix, f the volume fraction of the dielectric, and α is proportional to the polarizability. Under the assumption that ellipsoids are randomly oriented, the value for α is given by

$$\alpha=\frac{1}{3}\sum_{i=1}^{3}\frac{\epsilon_{\mathrm{mi}}-\epsilon_{\mathrm{ma}}}{\epsilon_{\mathrm{ma}}+D_i(\epsilon_{\mathrm{mi}}-\epsilon_{\mathrm{ma}})},$$

where the D_i are the triplets of the depolarization factors, ϵ_{mi} is the bulk dielectric constant of the less abundant constituent, and the $\frac{1}{3}$ factor is a consequence of assuming a random orientation of the ellipsoids. He then uses a log-normal distribution for the ratio of the major semiaxis a to the minor semiaxis c, a ratio that is directly connected to the D's, to calculate the effective dielectric constant of the cermets. Granqvist centered his log-normal distribution on a value of D that corresponds to the ratio $\langle a/c\rangle=8.7$; with this ratio he weighted he distribution towards oblate ellipsoids. Following this procedure, he obtained better agreement with experiment than when all the inclusions were assumed to be spheres.

Figure 2 illustrates the dependence of the imaginary part of the dielectric constant ϵ_2 on the depolarization factor D when it is varied from $0.2<D<1.0$. From the figure it can be seen that ϵ_2 is strongly dependent on the depolarization factor. Several distributions were used by us to perform the average, with the depolarization factors assuming values between 0.2 and 0.8, values that were considered to be consistent with observed micrographs. By taking a log-normal distribution with a D value centered at an average D value that corresponds to a ratio $\langle a/c\rangle=1$ (spheres), it was shown upon calculating the logarithm of the transmission that the result corresponds to the one obtained if only spheres had been used for the metallic inclusions. In fact, we were able to show that averaging over a distribution of shapes was not sensitive to the type of distribution or the average value of the a/c ratio used, unless a highly asymmetric distribution or one strongly weighted towards oblateness was utilized. We concluded that the average polarizability equals the value obtained for spherical grains as long as distributions consistent with observed micrographs are used. For this reason, it was decided that all multiple-scattering calculations would be performed only for spherical islands, since on the average, due to the random distribution in shape and orientation, the system behaves like a cermet made up of spherical islands.

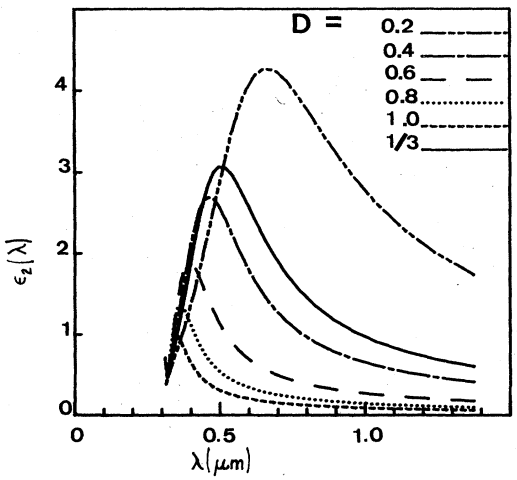

FIG. 2. Changes in the imaginary part of the dielectric constant due to the use of different depolarization factor D in the Maxwell-Garnett equation for the dielectric constant of Ag-MgO (80 vol % MgO).

II. SIZE CORRECTION TO THE DIELECTRIC CONSTANT OF THE METALLIC INCLUSIONS

A. Quantum size effects

In order to calculate the effective dielectric constant of cermets, it is necessary, in general, to correct the bulk dielectric constant of the minority constituent for size effects. Normally the insulator has a dielectric constant that is essentially frequency independent in the spectral range of interest, while the metallic constituent has a strong frequency dependence in the same region. When the metal is the minority constituent, its bulk dielectric constant must be corrected for size effects when the bulk mean free path becomes comparable to the size of the grains. Traditionally, the Drudes model together with experimentally obtained interband contributions is used to calculate the dielectric constant of the metal. In this procedure, the mean free path of the electrons in the metallic island is corrected for boundary scattering at the interface between the island and the external medium. Many researchers[12] have observed that in order to obtain a reasonably good fit between theory and experiment, it is necessary to use mean free paths that are considerably smaller than the ones attributed only to the size of the island. These corrections can be explained as the combination of boundary scattering at the metallic-grain surface and scattering inside the island due to internal imperfections and faults. Apparently, the contributions from these faults and imperfections is the dominant factor in determining the mean free path in most materials. This is not surprising since in many cases the formation process is based on the coalescence of small islands to form larger ones, a process that should produce substantial amounts of imperfections in the metallic grains. The Drude theory with these corrections is satisfactory for metallic grains of metals such as gold, silver, or copper with radii of more than 100 Å. However, when the size of the metallic particles become comparable to the electron wavelength, quantum corrections become mandatory if a realistic dielectric constant is to be obtained.

Until recently, no good theoretical models existed for calculating the dielectric constant of metallic particles with a radius of the order of 100 Å or less.[13] To solve this problem several researchers have used the quantum-box method within the random-phase approximation to calculate the dielectric constant of the metallic particles.

Kawabata and Kubo[14] have corrected the dielectric constant for size effects, assuming that the spectrum of the quantum levels form essentially a continuum, while Wood and Ashcroft[15] carefully reworked the quantum size method, fully taking into account the spectrum resulting from the box quantization, and obtained a dielectric constant for the particles that can be expressed as

$$\mathrm{Re}\epsilon(x)=1+\left[\frac{4}{\pi}\right]^4\frac{a}{a_0}\sum_{m=1}^{m_c}m^2(m_c^2-m^2)\sum_{m'=1}^{\infty}(m')^2[\Delta^2-(x^2+\Gamma^2)][1-(-1)^{m+m'}]/\Theta\ ,$$
$$\mathrm{Im}\epsilon(x)=\left[\frac{4}{\pi}\right]^4\frac{a}{a_0}\frac{\Gamma}{x}\sum_{m=1}^{m_c}m^2(m_c^2-m^2)\sum_{m'=1}^{\infty}(m')^2[\Delta^2+x^2+\Gamma^2][1-(-1)^{m+m'}]/\Theta\ , \tag{1}$$

where

$$\Theta=\Delta^3[(\Delta^2-x^2+\Gamma^2)^2+4x^2\Gamma^2],\quad \Delta=(m')^2-m^2$$
$$x=2\hbar\omega ma^2/\hbar^2\pi^2,\quad \Gamma=\hbar m_c^2/\tau\varepsilon_F,\quad m_c=I(K_Fa/\pi)\ .$$

ε_F is the Fermi energy, K_F the Fermi wave number, a is the size of the grains, a_0 the Bohr radius, and the function I takes the integer part of the argument.

Recently this formalism has been applied by the authors of this article to real cermets in the region where the metallic inclusions in the cermets are smaller than 100 Å (Ref. 16), and better results have been obtained for the dielectric constant than when the Drude model is used.

Figure 3 compares the imaginary part of the dielectric constant, taking into account quantum size effects (QSE's) following Wood and Ashcroft as expressed in Eq. (1), and the Kawabata and Kubo model (KK) with the one calculated using the Drude model. In the calculation of the Drude model the size of the silver particles is taken to be 30 Å and no interband contributions to the dielectric constant have been included. This model was corrected for size effect, using an effective relaxation time that correct the bulk result with boundary scattering through the relationship

$$1/\tau_{\mathrm{eff}}=1/\tau_b+V_F/a\ ,$$

where τ_b is the bulk relaxation time, V_F is the Fermi velocity, and a is the radius of the silver grains. The multiple peaks appearing in the QSE calculations are due to the discrete energy spectrum of an electron in a box. These peaks tend to decrease in magnitude as one moves from the infrared to the visible region of the spectrum.

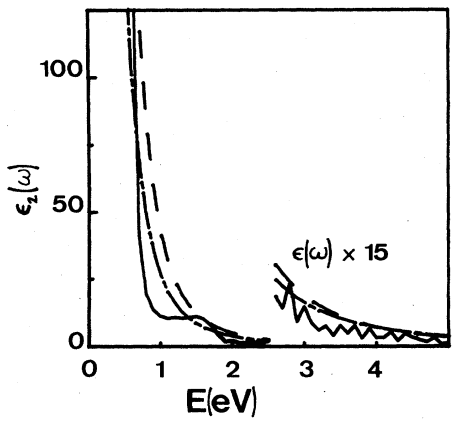

FIG. 3. Comparison between the imaginary part of the dielectric constant as a function of frequency for QSE, the solid curve; D, the dashed curve; and KK, the dashed-dotted curve.

Extensive computer calculations were made to compare the KK, QSE, and the Drude model for good metals such as silver, gold, and nickel, and it was found that in all cases, when the size of the islands exceeded 100 Å, the three models coincide in the value obtained for the dielectric constant of the metallic inclusions, provided that the KK model is corrected for a geometric factor of $\pi/6$.[17] For that reason the Drude formula, which is the simplest one, will be preferred for metallic islands of radii larger than this value.

B. Applications of the QSE to real cermets

We will now apply the QSE result to the calculation of the optical properties of real cermets and compare the results with those obtained using the Drude model. In this section interband contributions to the dielectric constant of the metal grains will be fully taken into account.[18] Experimentally, the resonances observed in the dielectric constant of an isolated metal grain due to quantum size effects are not observed in the effective dielectric constant of a real cermet. The disappearance of these peaks is due to the fact that the metallic grains in a real cermet do not have a unique size, but instead have a distribution of sizes as can be verified by micrographs of the materials. For this reason the dielectric constant obtained from the QSE calculations for one isolated particle was averaged over a distribution that realistically represented the variations in size of actual cermets.

If a histogram of the observed radii of the metallic grains is made, a distribution of the form illustrated in Fig. 4 is obtained, showing that the distribution is skewed towards large radii. The skewedness is consistent with the formation process of the inclusions, in which large particles are formed from smaller ones by coalescence. Actually, a log-normal distribution of the following form is usually used to fit the experimental results:[19]

$$f(R)=(1/\sqrt{2\pi})1/\sigma(\exp\{-1/2[\ln(R/R_0)/\sigma]^2\})\ ,$$

where R_0 is the average radius of the grains and σ is a measure of the width of the distribution and is given by $\sigma=\ln\sigma_{\ln}$. Experimentally, the value $\sigma_{\ln}$ is found to be between 1.1 and 1.5 for most cermets.[20] Averaging the dielectric constant of one metallic grain with a log-normal distribution function, an effective dielectric constant for the metallic grains in the cermet is obtained. This average QSE result is then used to calculate the effective-medium dielectric constant using the Bruggeman mean-field and multiple-scattering-correction theories.

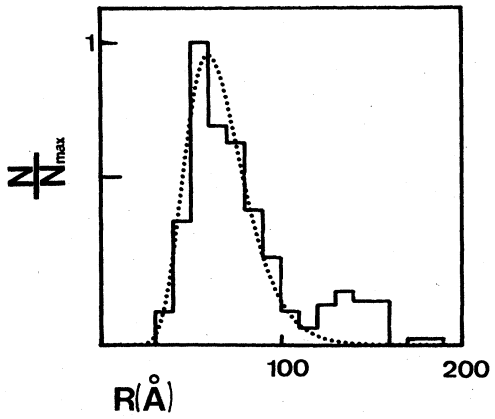

FIG. 4. Comparison between the experimentally obtained histogram (Ref. 21) and the log-normal distribution function of metallic-grain radii in a Ni-Al_2O_3 (20 vol % Al_2O_3) cermet with a geometrical standard deviation σ_{ln} of 1.3 and an average grain size of 30 Å.

In Fig. 5 the unaveraged and averaged quantum calculations are compared for a particle of average radius $R_0=30$ Å. As seen from the figure, the effect of taking the average with the log-normal distribution is to smooth out the quantum structure of a single particle when using the QSE approximation. Since experimentally the dielectric function of a cermet is found to be a smooth function of frequency, this is the correct dielectric constant to be used for the metal in calculating the effective dielectric constant of cermets. For radii in excess of 100 Å it is found, as expected, that the Drude and the averaged quantum results coincide.

Before applying these results to real cermets, it is important to discuss the relaxation-time concept as used in the Drude and the QSE methods. Usually the Drude model utilizes an effective relaxation time that corrects the bulk mean free path of the electrons for collisions with the grain walls. However, the relaxation time is not well understood for particles of radii below 100 Å. According to Wood and Ashcroft, surface-scattering corrections in terms of a mean-free-path concept are not appropriate when the presence of the surface actually determines the eigenstates of electrons within the particle's volume. The mean free path of electrons in the bulk metal for the case of silver is of the order of 100 Å, while for smaller metallic particles grown by sputtering processes, the mean free path is reduced due to imperfections within the metallic grain that result from the fabrication process. Small metallic inclusions in cermets are known to grow by coalescence of smaller inclusions which diffuse on the substrate and, as a result, a significant number of imperfections are trapped within the metallic grain during the formation process. To take into account the effect of these imperfections, we will introduce a restricted mean free path smaller than the bulk mean free path when applying the QSE calculation to obtain an effective complex dielectric constant.

We now compare with experimental data the results obtained when the QSE dielectric constant is introduced into

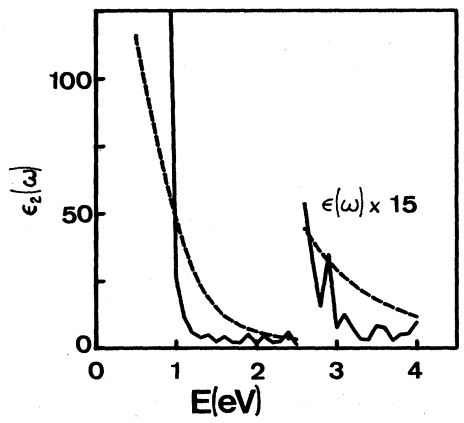

FIG. 5. Unaveraged and averaged QSE dielectric constant of Ag metallic grains for a grain distribution with average radius of 30 Å and a geometrical standard deviation of 1.3. Solid curve is the unaveraged value and the dashed curve the averaged one.

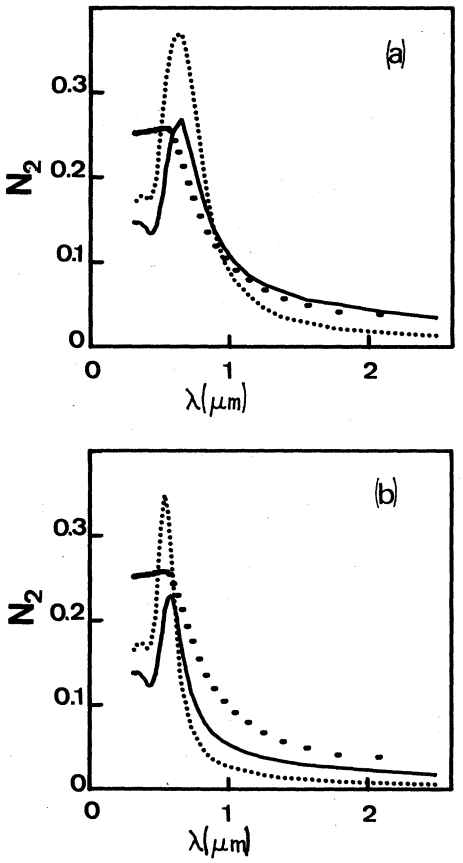

FIG. 6. Imaginary part of the index of refraction for Au-Al_2O_3 (90 vol % Al_2O_3). Interband contribution was taken from H. Ehrenreich *et al.* (Ref. 18). (a) compares BD, BQ, and experimental data (Ref. 21). (b) compares MGD, MGQ, and experimental data. Dotted curves are used for D, solid curves for the QSE model, and dots for experimental data.

the calculation of the effective dielectric constant of the cermet. The theoretical calculations will be compared with the measured refractive index for the Au-Al_2O_3 and Ag-MgO cermets obtained by Craighead.[21] This experimental data was selected because it is obtained from cermets with metallic grains of average radii less than 50 Å and, consequently, the QSE method should contribute significantly to the complex index of refraction.

Figure 6(a) compares the experimentally measured imaginary part of the complex index of refraction for Au-Al_2O_3 cermets with a 90% volume fraction of the dielectric constituent with the Bruggeman theory using the Drude model (BD), and with the Bruggeman theory using the QSE correction (BQ). The average radius for the calculations was taken to be 20 Å, and the value used for the limited mean free path was also 20 Å. As can be observed from the figure, the BD model exaggerates the magnitude of the observed resonance in the imaginary part of the index of refraction N_2. The BQ model greatly improves on the BD for N_2 by reducing the magnitude of the peak and approximating much better the actual values of N_2 in the infrared region of the spectrum. However, in this case there is no appreciable shifting of the position of the peak. Figure 6(b) shows the same experimental result for the Au-Al_2O_3 cermet but now compared with the Maxwell-Garnett theory, using for the metal the Drude dielectric constant (MGD) and the QSE (MGQ) values. As we have anticipated, MG predicts a too narrow and generally blue-shifted peak. In this case, QSE also reduces the magnitude of the peak, and a measurable red shift of the curve and a broadening effect is observed.

III. MULTIPLE-SCATTERING THEORIES

A. The first smoothing approximation

When thin films of cermets are grown by cosputtering or coevaporation methods, nucleation processes are responsible for the formation of metallic or dielectric islands in the matrix of the corresponding more abundant constituent. Since the nucleation process is governed by diffusion effects, relative island positions must be correlated. Several authors have developed a method to measure this correlation and demonstrated its existence.[22] The multiple-scattering theories developed here will assume that the islands of the minority constituent are correlated and that the corresponding correlation length is sufficiently large to make important contributions to the calculation. Thus, the purpose of the multiple-scattering calculations will be to correct the mean-field theories for the contribution of the correlation to the effective dielectric constant of the medium. It will be shown that these effects are important in obtaining a model with predictive value for the optical response of cermets.

The theory is based on the concept of a local dielectric constant that fluctuates around an average value ϵ_0 that is independent of position. This position-dependent dielectric constant can be written as

$$\epsilon(\mathbf{r},\omega)=\epsilon_0(\omega)+\delta\epsilon(\mathbf{r},\omega) ,$$

where $\delta\epsilon(\mathbf{r},\omega)$ corresponds to the spatially fluctuating term. The equation governing the electric field of the electromagnetic wave can then be written in terms of this spatially dependent dielectric constant as

$$\nabla\times\nabla\times\mathbf{E}-(\omega/c)^2\mu\epsilon\mathbf{E}-\mu^{-1}\nabla\mu\times\nabla\times\mathbf{E}=\mathbf{0} .$$

Rewriting this equation explicitly in terms of the fluctuating part of the dielectric constant, it can be expressed as

$$\nabla\times\nabla\times\mathbf{E}-K_0^2\mathbf{E}=K_0^2(\delta\epsilon/\epsilon_0)\mathbf{E} ,$$

where K_0 is the average propagation in a medium with average dielectric constant ϵ_0. In terms of operator formalism the field equation can be defined as a nonstochastic operator

$$H\equiv\nabla\times\nabla\times-K_0^2$$

and a stochastic term

$$H_1\equiv K_0^2(\delta\epsilon/\epsilon_0) .$$

The field equation then becomes

$$\mathbf{E}=\mathbf{E}_0+G_0H_1\mathbf{E} , \tag{2}$$

where $\mathbf{E}_0$ is the electric field that results from solving the nonstochastic operator. Since we are in the presence of a random medium and we will assume that an effective-medium dielectric constant can be defined, an average of this equation can be performed to obtain

$$\langle\mathbf{E}\rangle=\mathbf{E}_0+G_0\langle H_1\mathbf{E}\rangle .$$

From this expression an infinite multiple-scattering expansion in terms of H_1 can be performed with the condition that the fluctuating term is centered around the averaged dielectric constant and therefore $\langle H_1\rangle=0$. Diagrammatically this expansion can be represented as follows:

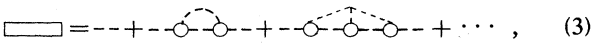 , (3)

where the dashed line represents the Green's function associated with $\mathbf{E}_0$, the rectangle represents the Green's function associated with $\langle\mathbf{E}\rangle$, and the open circle represents H_1. The dashed line indicates correlation between local scattering points. The above equation, although exact, cannot be solved. In order to be able to obtain useful values for the effective dielectric constant, the first smoothing approximation (FSA),[23,24] which only takes into consideration pair-correlation functions, will be used. This approximation yields the equation

$$\mathbf{E}=\mathbf{E}_0+G_0\langle H_1G_0H_1\rangle\langle\mathbf{E}\rangle ,$$

which upon interaction can be expressed diagrammatically as

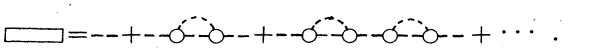 .

This diagram contains the pair correlation functions

$$\langle\delta\epsilon(\mathbf{r}_1)\delta\epsilon(\mathbf{r}_2)\rangle$$

represented by the dashed lines. Following the procedure of Karal and Keller,[25] this approximation was used to obtain an effective-medium dielectric constant ϵ_{eff}. To do

this, it was necessary to assume a plane-wave solution for the macroscopic field with an effective propagation constant

$$K^2 \equiv (\omega/c)^2 \epsilon_{\text{eff}} .$$

Previous work by the present authors[26] indicates that the pair correlation can be expressed as an exponential relationship with a correlation length L in the following form:

$$\langle \delta\epsilon(\mathbf{r}_1)\delta\epsilon(\mathbf{r}_2)\rangle = \Delta e^{-r/L} ,$$

$r = |\mathbf{r}_2 - \mathbf{r}_1|$, and Δ is shown to be well represented by the square of the standard deviation of the fluctuations. In the spectral range of interest the final dispersion relation becomes

$$\epsilon_{\text{eff}} = \epsilon_0 + \frac{\Delta}{2\epsilon_0}\left[\frac{2}{3} + \frac{1+ia}{a^2} + \frac{2a^2}{1-i2a} - \left[\frac{1}{a} + \frac{1+a^2}{a^3}\right]\cot^{-1}\left[\frac{1-ia}{a}\right]\right] ,$$

where

$$a^2 \equiv \epsilon_0 \omega^2 L^2/c^2 .$$

The new effective dielectric constant includes the averaged dielectric constant plus a term that is a function of the correlation length L. This calculation is conceptually based on the assumption that there is an averaged dielectric constant around which local fluctuations due to the metallic and dielectric islands occur and is known as the random-continuum model. Since this is precisely the model that is described by the Bruggeman theory, we have chosen as the averaged dielectric constant ϵ_0, the one obtained from that theory. This is perfectly consistent with multiple-scattering theory since it can be shown that the Bruggeman model is a zeroth-order approximation of multiple-scattering theories. The proof consists in assuming that both the metallic and the dielectric constituents form spherical scattering sources in an average medium, and then, in the absence of correlation, the average of the T matrix $\langle T\rangle$ can be written as the volume fraction average of the single-metal-particle T matrix T_1 and the dielectric-particle T matrix T_2 as $\langle T\rangle = fT_1 + (1-f)T_2$, where f is the volume fraction. Then taking the long-wavelength limit and assuming the self-consistent condition $\langle T\rangle = 0$, the Bruggeman equation is immediately obtained.

The theoretical predictions of both the Bruggeman and FSA models will now be compared with experimental data for Ag-MgO, 80 vol% MgO, and Au-Al_2O_3, 84 vol% Al_2O_3. Figures 7(a) and 7(b) show the imaginary parts of the index of refraction of these cermets. For the calculation, as presented in Fig. 7(a), the dielectric constant of the metallic islands was obtained from the Drude model corrected for a restricted mean free path due to size effects and due to impurities and defects. As observed, the Bruggeman model predicts higher values for the imaginary part of the index of refraction, N_2, than those obtained experimentally, whereas the FSA model fits the experimental data very well in almost all the region in the case of Ag-MgO where the radius of the islands is of the order of 80 Å and a restricted mean free path of 5 Å is used. In the case Au-Al_2O_3, it is necessary to make quantum corrections in order to obtain the best fit because the islands in this case are of the order of 30 Å. In this second case, the resonance in the imaginary part of N_2 is shifted towards longer wavelengths with respect to the experimental results.

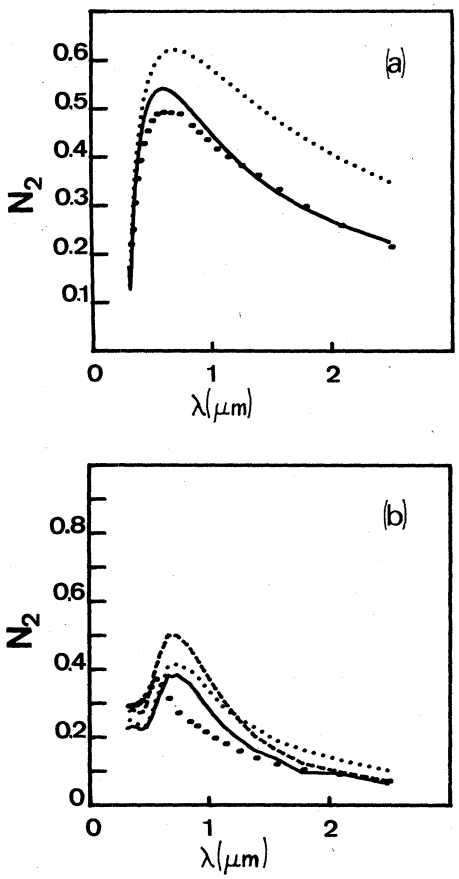

FIG. 7. Comparison between experimental data (Ref. 21) and calculations for N_2. (a) Ag-MgO (80 vol % MgO) cermet compared with B (dotted curve) and FSA (solid curve) model with $L = 125$ Å, and a restricted mean free path of 10 Å. (b) Au-Al_2O_3 (84 vol % Al_2O_3) cermet compared with BD (dashed curve), BQ (dotted curve), and FSAQ (solid curve) models with $L = 80$ Å, $a = 30$ Å, and restricted mean free path of 10 Å.

B. Renormalized FSA approximation

The results obtained using the QSE and multiple-scattering corrections in the FSA approximation to the B model show improvements on the predicted value for the imaginary index of refraction, but these corrections, although they affect the magnitude of the resonance, do not broaden or shift the resonance peak. In general, the B and MG models do not predict correctly the position nor width of the absorption peak. This suggests that a renor-

malized approach to the multiple-scattering calculation may be the correct path toward obtaining the necessary corrections to the position and width of the resonance peak. A renormalized procedure can be devised[24] starting from the field equation (3) and then using a T-matrix calculation for single spherical scatterers. Contrary to the case of the FSA approximation, the cermet is conceived here as spherical islands of the minority constituent embedded in a matrix of the dominant constituent. Each one of these spherical islands is then taken to be a scattering source from which the overall scattering wave for the random medium can be obtained. Since this model of the cermet is consistent with the MG model, the whole procedure will be constructed on a zeroth-order scattering dielectric constant that is obtained from a MG theory, thus assuming a noncorrelated medium in which the spherical grains serve as scattering sources. Equation (2) can be written in diagrammatic form as

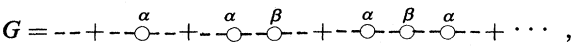

(4)

where the superscripts on each point refer to a specific scatterer that produces a local fluctuation H_1 in the background medium. The single-scattering T matrix is defined as

$$T_\alpha \mathbf{E}_0 = H_{1\alpha}\mathbf{E}$$

or

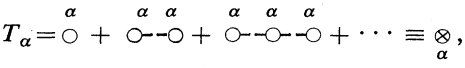

where the symbol $\otimes$ represents the new renormalized potential for single-scattering spherical sources. In terms of this new renormalized potential, Eq. (4) becomes

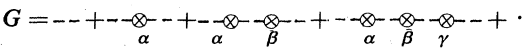

Naturally, in this equation the subscripts cannot be identical on two consecutive points since these terms have already been taken into account in the single-particle-scattering T matrix. If the statistical average is performed on this Green's function, the following statistically averaged Green's function is obtained:

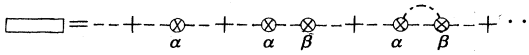

This expression contains both correlated and uncorrelated terms. A renormalized propagator that only takes into account uncorrelated terms is then defined as

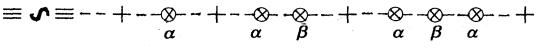

where G_0' is the renormalized uncorrelated Green's function identified with the propagation of an electromagnetic wave in an uncorrelated medium. In terms of the renormalized Green's function and scattering potentials, the general correlated Green's function can be expressed as

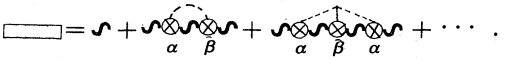

This expression is formally equivalent to the random-continuum final equation (3) that was used in the FSA approximation with the difference that now the scattering sources $\otimes_\alpha$ and the intermediate propagation Green's functions have been renormalized taking into account all uncorrelated terms. A simple correspondence can be made between the previous and the present equation through the following symbolic equivalences:

$$\text{---}\rightarrow\sim, \quad \text{that is,} \quad G_0 \rightarrow G_0' ,$$

$$\circ \rightarrow \otimes, \quad \text{that is,} \quad H_1 \rightarrow T .$$

As previously stated, in the absence of correlation effects or, equivalently, in an uncorrelated medium, a zeroth-order dielectric constant is obtained that corresponds to the MG model.[10] Applying now the first smoothing approximation to this diagram, which is equivalent to neglecting all correlations higher than the two-point correlation and also neglecting unlinked and nested two-point correlations, yields an equation that is formally equivalent to the FSA but renormalized and written in the following form:

$$\langle \mathbf{E} \rangle = \mathbf{E}_0 + G_0' \langle T G_0' T \rangle \langle \mathbf{E} \rangle ;$$

diagrammatically this can be written as

(5)

where $\langle \mathbf{E}_0 \rangle$ is the statistically averaged field propagating in the uncorrelated medium and $\langle \mathbf{E} \rangle$ the effective total field. The second term on the right-hand side this self-consistent equation represents scattering processes where the effective total field $\langle \mathbf{E} \rangle$ is scattered by pairs of correlated islands α and β located, respectively, at $\mathbf{r}_i$ and $\mathbf{r}_j$. In order to apply this formalism, an explicit mathematical representation of the diagram in the second term of the right-hand side of Eq. (5) must be obtained. Peterson and Strom[27] developed a formalism to obtain the T matrix for an array of n scattering objects with well defined spatial coordinates. Their formalism is an extension to a multiple number of scatterers of the one developed by Waterman[28] for a single scatterer. In Waterman's formalism, the T matrix for a single scatterer is obtained expanding all the local fields in terms of spherical harmonics and Bessel or Hankel functions. The term describing this double-scattering process in the Peterson-Strom formalism is given by

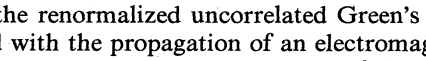

(6)

where T^α and T^β are the single-scatterer T matrices of islands α and β, respectively, expressed with their center at the origin of the coordinate system. The formalism then translates the particle through matrices R and σ to their correct position $\mathbf{r}_i$ and $\mathbf{r}_j$. Expressions for T^α are described in several articles,[27,28] and expressions for matrices R and σ can be found in the article of Peterson and Strom.[27] Using Eq. (2), the field equation can now be expressed as

$$\langle \mathbf{E}(\mathbf{r})\rangle=\langle \mathbf{E}_0(\mathbf{r})\rangle+(1/V^2)\sum_{\substack{\alpha,\beta\\(\beta\neq\alpha)}}\int\int g(\mathbf{r}_i,\mathbf{r}_j)R(\mathbf{r}_j)T^{\alpha}\sigma(\mathbf{r}_i-\mathbf{r}_j)T^{\beta}R(\mathbf{r}_j-\mathbf{r}_i)R(-\mathbf{r}_j)\langle \mathbf{E}\rangle d\mathbf{r}_i d\mathbf{r}_j\ , \tag{7}$$

where $g(\mathbf{r}_i,\mathbf{r}_j)$ is the two-point correlation function and V is the volume of the film. Considering the spheres as impenetrable and the medium as isotropic, an exponential metal-metal correlation function can be defined as

$$g(\mathbf{r}_i,\mathbf{r}_j)=\Theta(r-2a)\exp(-|\mathbf{r}_i-\mathbf{r}_j|/L)\ ,$$

where Θ is the Heaviside function, L the correlation length, and the correlation function measures the excess of the metal density with respect to its average; for this reason the function goes to zero at large distances. To simplify the calculation we assume all the metallic grains to be spherical in shape and of equal radius, which allows us to write $T^{\alpha}=T^{\beta}$ and make them diagonal matrices. Assuming a macroscopic volume, we can replace $(1/V^2)\sum$ by δ^2, where δ is the density of islands in the cermet. With this approximation the field equation can be written as

$$\langle \mathbf{E}(\mathbf{r})\rangle=\langle \mathbf{E}_0(\mathbf{r})\rangle+\delta^2\int d\mathbf{r}_j R(\mathbf{r}_j)\int_{1>2a} dl\exp(-|l|/L)T\sigma(l)TR(-l)R(-\mathbf{r}_j)\langle \mathbf{E}\rangle\ ,$$

where the substitution $l\equiv\mathbf{r}_i-\mathbf{r}_j$ has already been performed. The field $\langle \mathbf{E}\rangle$ and $\langle \mathbf{E}_0\rangle$ will be expanded in terms of the basis functions $\{\psi_n^{\mathrm{reg}}(K_0\mathbf{r})\}$ that are regular solutions to the Helmholtz equation described by Waterman.[28] The ψ_n are known as the elementary fields and K_0 is the propagation constant of the electromagnetic wave in the zeroth-order effective medium. In terms of this basis the fields can be expressed as

$$\langle \mathbf{E}_0\rangle=\sum_n d_n\psi_n^{\mathrm{reg}}(K_0\mathbf{r})$$

and

$$\langle \mathbf{E}(\mathbf{r})\rangle=\sum_n X_n\psi_n^{\mathrm{reg}}(K_0\mathbf{r})\ ,$$

while the total effective field $\langle \mathbf{E}\rangle$ in the second term of the right-hand side is expanded in a base centered at one of the correlated islands:

$$\langle \mathbf{E}\rangle=\sum_n B_n\psi_n^{\mathrm{reg}}(K_0(\mathbf{r}-\mathbf{r}_j))\ .$$

Substituting these expansions for the fields in Eq. (7) and performing the integration over the relative coordinate between correlated islands, we obtain

$$\sum_n X_n\psi_n^{\mathrm{reg}}(K_0\mathbf{r})=\sum_n d_n\psi_n^{\mathrm{reg}}(K_0\mathbf{r})+\delta^2\sum_n M_n\int B_n\psi_n(K_0(\mathbf{r}-\mathbf{r}_j))d\mathbf{r}_j\ . \tag{8}$$

Matrix elements M_n contain all the correlation effects and can be written in terms of the elements of the single-scatterer T matrix. Since the wavelength of incident radiation relevant to our problem is $\lambda>0.3\ \mu$m and the radii of islands for typical cermets are of the order of $0.01\ \mu$m, the long-wave limit can be utilized, thus reducing the expansion of the electromagnetic field to the magnetic and electric dipolar terms. In this limit only the first six terms of these matrices are necessary:

$$M_1=M_3=M_5=A_1T_1^2+A_2T_1T_2\ ,$$

$$M_2=M_4=M_6=A_1T_2^2+A_2T_1T_2\ ,$$

where

$$A_1\cong-(22\pi i/5K_0)(L^2+2aL)\exp(-2a/L)\ ,$$

$$A_2\cong(5/11)A_1\ ,$$

$$T_1\cong i(2/15)(K_0a)^5(1-\epsilon_r)\ ,$$

$$T_2\cong i(2/3)(K_0a)^3(\epsilon_r-1)/(\epsilon_r+2)\ .$$

ϵ_r is the ratio of the dielectric constants of the metallic islands and the external medium, and it represents the source of the multiple-scattering processes. To perform the integral over the $\mathbf{r}_j$ coordinate, the properties of the translation matrices[29] σ must be used to displace the ψ_n from position $\mathbf{r}_j$ to the origin:

$$\psi_n(K_0(\mathbf{r}-\mathbf{r}_j))=\sum_{n'}\sigma_{n'n}(K_0\mathbf{r}_j)\psi_{n'}^{\mathrm{reg}}(K_0\mathbf{r})\ ,$$

then Eq. (8) reduces to

$$\sum_n X_nR_e\psi_n(K_0\mathbf{r})=\sum_n d_n\psi_n^{\mathrm{reg}}(K_0\mathbf{r})+\delta^2\sum_{n,n'}M_n\int B_n\sigma_{n'n}(K_0\mathbf{r}_j)\psi_{n'}^{\mathrm{reg}}(K_0\mathbf{r})d\mathbf{r}_j\ . \tag{9}$$

All terms in Eq. (9) are now written in the same orthogonal basis and, therefore, can be reduced to an equivalent set of scalar equations:

$$X_n=d_n+\delta^2\sum_{n'}\int M_{n'}B_{n'}\sigma_{nn'}d\mathbf{r}_j\ .$$

The limits of integration in the above expression must be restricted to values $|\mathbf{r}_j-\mathbf{r}|>a$ in order to avoid having the scattered field inside the scattering island located at $\mathbf{r}_j$. Since in the long-wave limit the electromagnetic wave tends to average the microstructure at the scale of island sizes, it can be assumed that the wave propagates in the effective medium as a plane wave. The coefficient d_n representing the unperturbed wave can be written in terms of the effective propagation constant K_0 as

$$d_n=d_n^0\exp(i\mathbf{K}_0\cdot\mathbf{r})\ ,$$

while the coefficient representing the total average field $\langle \mathbf{E}\rangle$ can also be expressed in terms of the effective propa-

gation constant K of the correlated medium as

$$X_n = X_n^0 \exp(i\mathbf{K}\cdot\mathbf{r})$$

and

$$B_n = X_n^0 \exp[i\mathbf{K}\cdot(\mathbf{r}-\mathbf{r}_j)] .$$

In terms of these expressions the field equation now becomes

$$X_n^0 \exp(i\mathbf{K}\cdot\mathbf{r}) = d_n^0 \exp(i\mathbf{K}_0\cdot\mathbf{r}) + \delta^2 \sum_{n'} M_{n'} X_{n'}^0 \int_{|\mathbf{r}-\mathbf{r}_j|>a} \exp[i\mathbf{K}\cdot(\mathbf{r}-\mathbf{r}_j)]\sigma_{nn'}(K_0\mathbf{r}_j)d\mathbf{r}_j .$$

Following the procedure described by Varadan *et al.*,[10] the scalar Helmholtz operator can be used in the zeroth-order approximation to simplify the above equation and reduce the volume integral to a surface integral:

$$X_n^0 = \sum_n M_{n'} X_{n'}^0 I_{nn'} , \tag{10}$$

where

$$I_{nn'} = \delta^2/(K^2-K_0^2)\int_{|\mathbf{r}|>a} \left[\sigma_{nn'}(-K_0\mathbf{r}) \frac{\partial \exp(i\mathbf{K}\cdot\mathbf{r})}{\partial r} - \exp(i\mathbf{K}\cdot\mathbf{r}) \frac{\partial \sigma_{nn'}(-K_0\mathbf{r})}{\partial r} \right] ds .$$

Equation (10) represents a system of homogeneous coupled equations with unknown coefficients. By solving the associated secular equation, a new dispersion relationship was obtained that took into account pair correlations in the scattering medium:

$$K^2 - K_0^2 = (-i\pi\delta^2 M_6/K_0)[2+(K/K_0)^2] .$$

In terms of the dielectric constants this expression can be written as

$$\epsilon = \bar{\epsilon}_0(1+2Fk^2\epsilon_0)/(1-Fk^2\epsilon_0) , \tag{11}$$

where ϵ is the new effective dielectric constant in the correlated medium of the film obtained from the renormalized FSA model, $k=\omega/c$ is the propagation constant of the electromagnetic wave in vacuum, and F contains all the effects due to correlations between islands and its explicit form is

$$F = \tfrac{22}{50} f^2 \exp(-2a/L)(L^2+2aL)[(\epsilon_r-1)/(\epsilon_r+2)]^2 .$$

IV. RESULTS AND CONCLUSIONS

The classical approach to the theory of the optical properties of cermets has traditionally used the Drude model corrected for interband transitions to obtain the complex dielectric constant of the metallic constituent with an effective relaxation time that takes into account surface scattering but fails to consider quantum effects. From the present work, it is evident that this approach is valid when the radii of the metallic inclusions are larger than 100 Å and when the metals used are good metals. We have shown that when the radii of the metallic grains are smaller than 100 Å, QSE become an important correction to the effective dielectric constant of the metallic grains when calculating the optical properties of cermets. When using the QSE results, it is necessary to average the discrete absorption peaks with a log-normal distribution of island sizes. This average is necessary, since experimentally no structure is observed in measured optical constants of cermets. In general, the ability to reproduce the experimentally observed optical properties of cermets is considerably improved when the dielectric constant of the metallic constituents for islands less than 100 Å is corrected for quantum size effects.

The next step to improve the calculation of the optical properties of cermets is to include two-point correlation between neighboring grains. Under this condition a multiple-scattering theory must be developed that will take into account interference effects between the scattering produced by neighboring metallic grains that are correlated. In order to simplify the multiple-scattering correction, the first smoothing approximation was used, thus limiting the calculation to pair correlations through a self-consistent equation. In performing this calculation, an average dielectric constant is assumed that is conceptually compatible with the B model of a cermet. Multiple-scattering corrections in the FSA approximation, with a metallic dielectric constant corrected for QSE in the cases where the islands are smaller than 100 Å, were shown to improve the predicted value of the B theory but were unable significantly to shift the position or broaden the resonance peak of the complex index of refraction. For this reason, it was considered necessary to improve further the calculation by taking into account renormalized effects in a T-matrix context. The result of this calculation, shown in Eq. (11), permits the calculation of the complex effective dielectric constant of cermets, taking into account correlation effects that include renormalization corrections. This equation is expressed in terms of the following basic physical parameters obtainable from experimental data: the average radius of the metallic island a, the correlation length L, the volume fraction of the metallic constituents f, the bulk dielectric constant of the metallic grains ϵ_m, and the bulk dielectric constant of the dielectric material. As the metallic concentration is reduced, the correlation length tends to vanish and we recover from Eq. (11) the zeroth-order approximation $\bar{\epsilon}_0$, the effective dielectric constant of the uncorrelated medium. Since in the renormalized calculation, islands of the minority constituent are assumed to be the scattering sources embedded in a medium of the majority constituent, the proper

starting zeroth-order-approximation dielectric constant is the MG one.

As previously stated, the bulk metallic dielectric constant must be corrected for size effects for islands of 100 Å or less. We have applied this refined calculation to Ag-MgO and Ni-Al_2O_3 cermets where experimental data is available from the work of Craighead.[21] The volume percentage of metallic constituent is 20% in Ag-MgO and between 39% and 46% in Ni-Al_2O_3. These concentrations are considered to be high and are normally not predicted well by mean-field theories. Since as metal concentration increases correlation effects become more important, it is expected that multiple-scattering effects should be more significant in these high-concentration regimes. In making the calculations, the average radius of the islands were estimated and the mean free path and correlation length were then adjusted to obtain the best fit with experiment. When the Drude model was used in the Ag-MgO cermet [Fig. 8(a)], it was necessary to utilize a 3-Å mean free path in order to obtain the best fit with the experimental imaginary index of refraction. This was considered to be too short a mean free path, even after taking into account the fact that silver tends to have a large number of internal imperfections as mentioned by H. Craighead.[21] In the calculation, the optimal radius for the metallic islands was 80 Å, a value considered to be somewhat small according to estimates made from micrographs. An improvement in this calculation was obtained when the average radius of 125 Å for the islands was used and the QSE corrections were made [Fig. 8(b)]. For this case, the shift in the peak was in good agreement but relatively narrow compared to the experimental results. In both cases the correlation length was equal to six islands, a value that is compatible with experimentally measured correlations in other cermets.

The main conclusion that can be obtained from this calculation is that our renormalized FSA theory makes the best correction to the MG mean-field theories. It is possible to adjust the three adjustable parameters to obtain better fits, but what is significant is that all values are compatible with experimentally known facts.

Figure 9 is a similar comparison for Ni-Al_2O_3 with me-

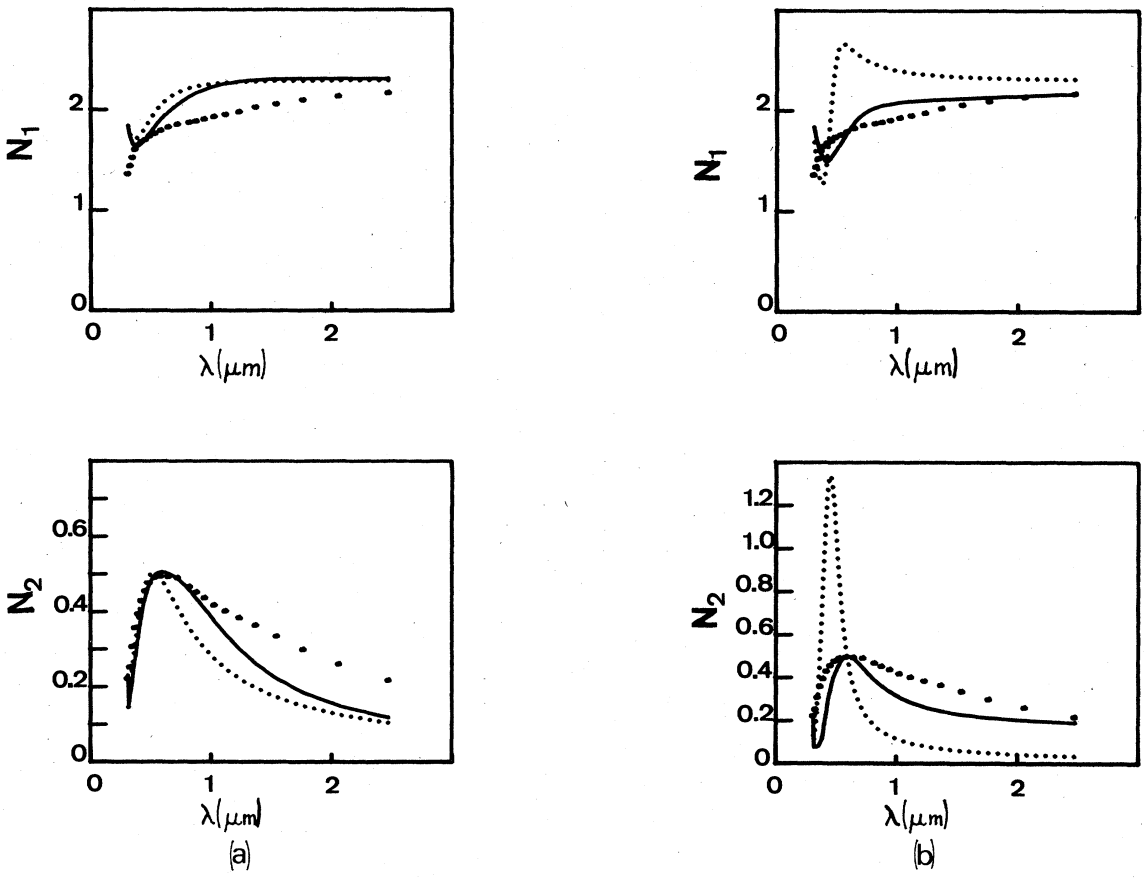

FIG. 8. Real (N_1) and imaginary (N_2) part of the refractive index is drawn for a Ag-MgO (80 vol % MgO) cermet. Solid curve is the renormalized FSA calculation, dotted curves represent the MG model, and dots are for the experimental results (Ref. 21). (a) N_1 and N_2 using the D model with $\tau=2.14\times10^{-16}$ s in both MG and renormalized FSA. The radius of the islands is taken as 80 Å and $L=6$ islands. (b) N_1 and N_2 using QSE with a restricted mean free path of 10 Å for dielectric constant of the metallic grains. The island radius is taken to be 125 Å and $L=6$ islands.

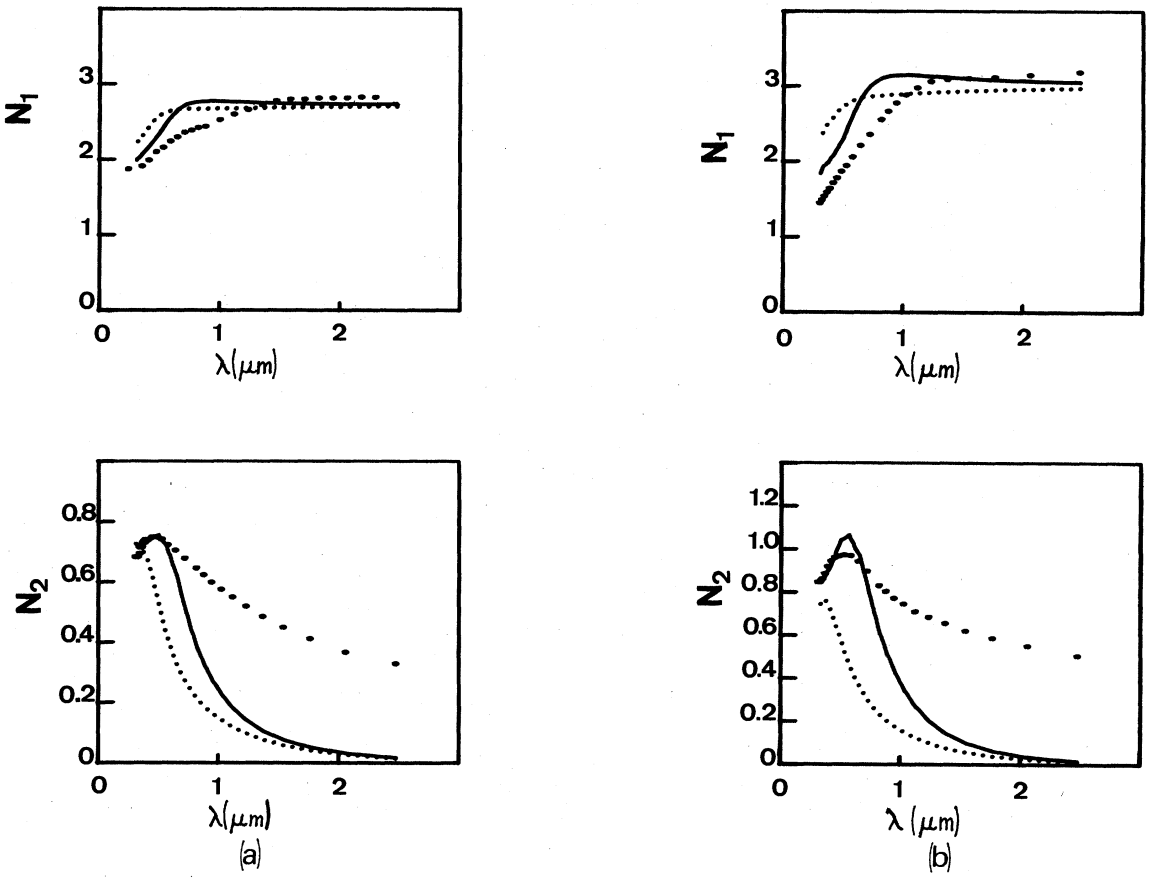

FIG. 9. Real and imaginary part of the index of refraction for Ni-Al_2O_3, dotted curve is MGD, solid curve is renormalized FSA, and dots are experimental results (Ref. 21). (a) 61 vol% Al_2O_3 with $\tau=5.6\times10^{-16}$ s, $a=60$ Å, and $L=4$ islands. (b) 54 vol% Al_2O_3 with $\tau=3.5\times10^{-16}$ s, $a=75$ Å, and $L=4$ islands.

tallic concentrations of 39 and 46 vol%. Very good agreement for the position of the resonance peak and overall width was achieved with a reasonable value for the mean free path of 10 Å, and with radii consistent with the micrographs.[21] The fit between theory and experiment obtained in this figure is particularly significant, since the metallic concentrations used are close to, if not within, the percolation regime, a region where the mean-field models totally fail to reproduce experimental results. Probably this regime is close to the limit of concentrations for which the renormalized FSA approximation will be valid since we do not expect our calculations to be applicable in the percolation region.

The results of this and another recent paper[26] lead us to conclude that correlation effects and multiple-scattering corrections make important contributions to the optical properties of cermet materials and need to be included in theories with predictive value. Equation (11) is restricted to spherical shapes in the long-wave limit, but the formalism as presented here can be extended to include other island shapes and to permit corrections for higher multipolar contributions to the field equation. These multipolar corrections may become important when the metal concentration increases to the point that island proximity is no longer compatible with the dipolar approximation. The proposed dispersion relations depend strongly on the model used for the zeroth-order dielectric constant and the values used for the dielectric constant of the metallic grains. Other zeroth-order models for the effective-medium dielectric constant are being studied as possible starting points for the application of the dispersion relationships presented in this paper. These new calculations may permit the use of a longer and more realistic mean free path. Recently, other models have been developed for $\bar{\epsilon}_0$ that could help moderate the height and broaden the resonance with larger values for the mean free path.[30]

ACKNOWLEDGMENT

This work was supported by the U.S. Army Research Office through Grant No. DAAG-29-81-G0010.

*On leave from Escuela de Física, Universidad de Costa Rica, Costa Rica.
†Present address: Cornell University, Ithaca, NY 14853.

[1]A. J. Sievers, in Proceedings of the Advanced Research Projects Agency Materials Research Council Summer Conference, La Jolla, California, 1974, Vol. 2, p. 245 (unpublished).
[2]B. Abeles and J. I. Gittleman, Appl. Opt. **15**, 2328 (1976).
[3]B. Abeles, P. Sheng, M. D. Coutts, and Y. Arie, Adv. Phys. **24**, 407 (1975).
[4]See, for example, J. D. Jackson, *Classical Electrodynamics* (Wiley, New York, 1975).
[5]These two models are described elsewhere. The original papers are J. C. Maxwell-Garnett, Philos. Trans. R. Soc. London **203**, 385 (1904); D. A. Bruggeman, Ann. Phys. (Leipzig) **24**, 636 (1935).
[6]C. G. Granqvist, J. Phys. (Paris) Colloq. **42**, C1-247 (1981).
[7]G. B. Smith, J. Phys. D **10**, L39 (1977).
[8]G. A. Niklasson, C. G. Granqvist, and O. Hunderi, Appl. Opt. **20**, 26 (1981).
[9]J. E. Gubernatis, in *Proceedings of the First Conference on the Electrical Transport and Optical Properties of Inhomogeneous Media, Ohio State University, 1977,* edited by J. C. Garland and D. B. Tanner (AIP, New York, 1978).
[10]V. K. Varadan, V. N. Bringi, and V. V. Varadan, Phys. Rev. D **19**, 480 (1979).
[11]R. W. Cohen, G. D. Cody, H. D. Coutts, and B. Abeles, Phys. Rev. B **8**, 3689 (1973).
[12]See, for example, Ref. 11.
[13]M. Cini, J. Opt. Soc. Am. **71**, 386 (1981).
[14]A. Kawabata and R. Kubo, J. Phys. Soc. Jpn. **21**, 1765 (1966).
[15]D. M. Wood and N. W. Ashcroft, Phys. Rev. B **25**, 6255 (1982).
[16]M. Gómez, G. Rodríguez, and L. Fonseca, Ferroelectrics **54**, 223 (1984); **54**, 227 (1984).
[17]R. Ruppin and H. Yatom, Phys. Status Solidi B **74**, 647 (1976).
[18]H. Ehrenreich and H. R. Philipp, Phys. Rev. **128**, 1622 (1962).
[19]C. G. Granqvist and R. A. Buhrman, J. Appl. Phys. **47**, 2220 (1976).
[20]J. M. Gerardy and M. Ausloos, Phys. Rev. B **26**, 4703 (1982).
[21]H. Craighead, Ph.D. thesis, Cornell University, 1980.
[22]P. B. Corson, J. Appl. Phys. **45**, 3165 (1974).
[23]R. C. Bourret, Nuovo Cimento **26**, 1 (1962).
[24]U. Frisch, in *Probabilistic Methods to Applied Mathematics,* edited by A. T. Bharucha-Reid (Academic, New York, 1968), p. 75.
[25]F. C. Karal and J. B. Keller, J. Math. Phys. **5**, 537 (1964).
[26]M. Gómez, L. Fonseca, and G. Rodríguez, Ferroelectrics Lett. **2**, 17 (1984).
[27]B. Peterson and S. Strom, Phys. Rev. D **8**, 3661 (1973).
[28]P. C. Waterman, Phys. Rev. D. **3**, 825 (1971).
[29]V. V. Varadan, in *Acoustic Electromagnetic and Elastic Wave Scattering,* edited by V. K. Varadan and V. V. Varadan (Pergamon, New York, 1979), p. 48.
[30]A. Liebsch and B. N. J. Persson, J. Phys. C **16**, 5375 (1983).